

Supporting Information

Design of photoinitiator-functionalized hydrophilic nanogels with uniform size and excellent biocompatibility

Meng Wei,^{ab} Yanjing Gao,^b Shengling Jiang,^c Jun Nie^{ab} and Fang Sun^{*ab}

^a State Key Laboratory of Chemical Resource Engineering, Beijing University of Chemical Technology, Beijing 100029, People's Republic of China

^b College of Science, Beijing University of Chemical Technology, Beijing 100029, People's Republic of China

^c College of Materials Science and Engineering, Beijing University of Chemical Technology, Beijing 100029, People's Republic of China

*Corresponding Author: E-mail:sunfang60@yeah.net, Phone:+86-10-64449336, Fax: +86-10-64437802

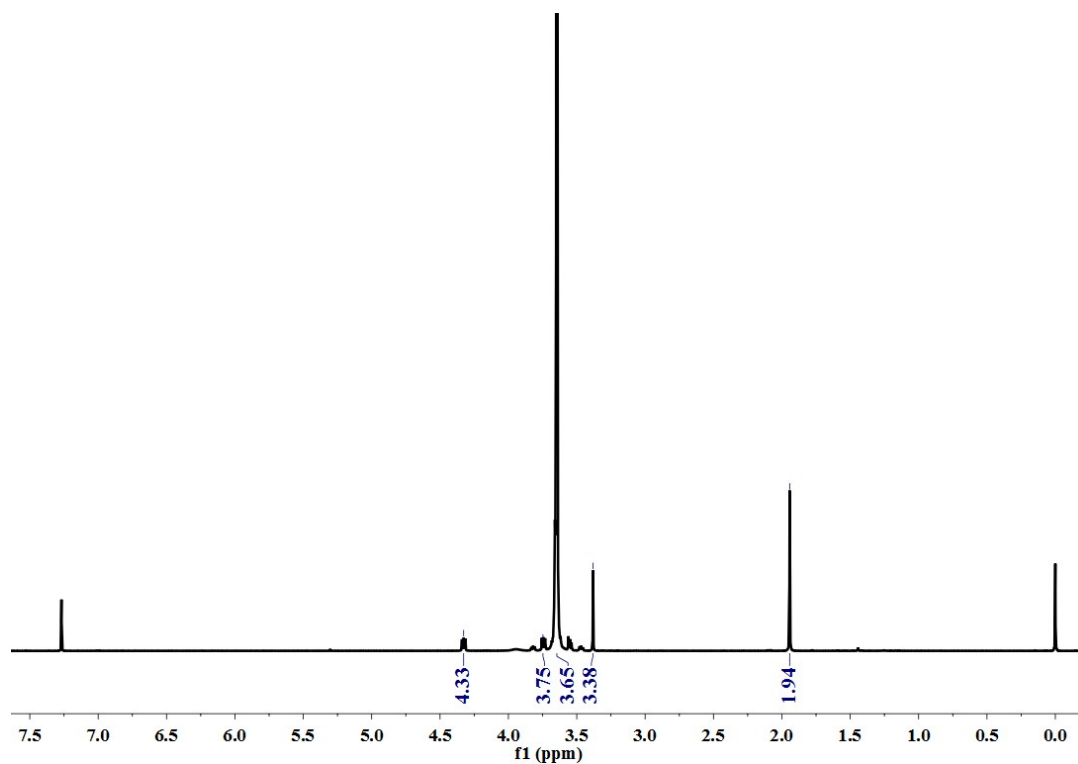


Figure S1. ¹H NMR spectrum of PEO5000-Br

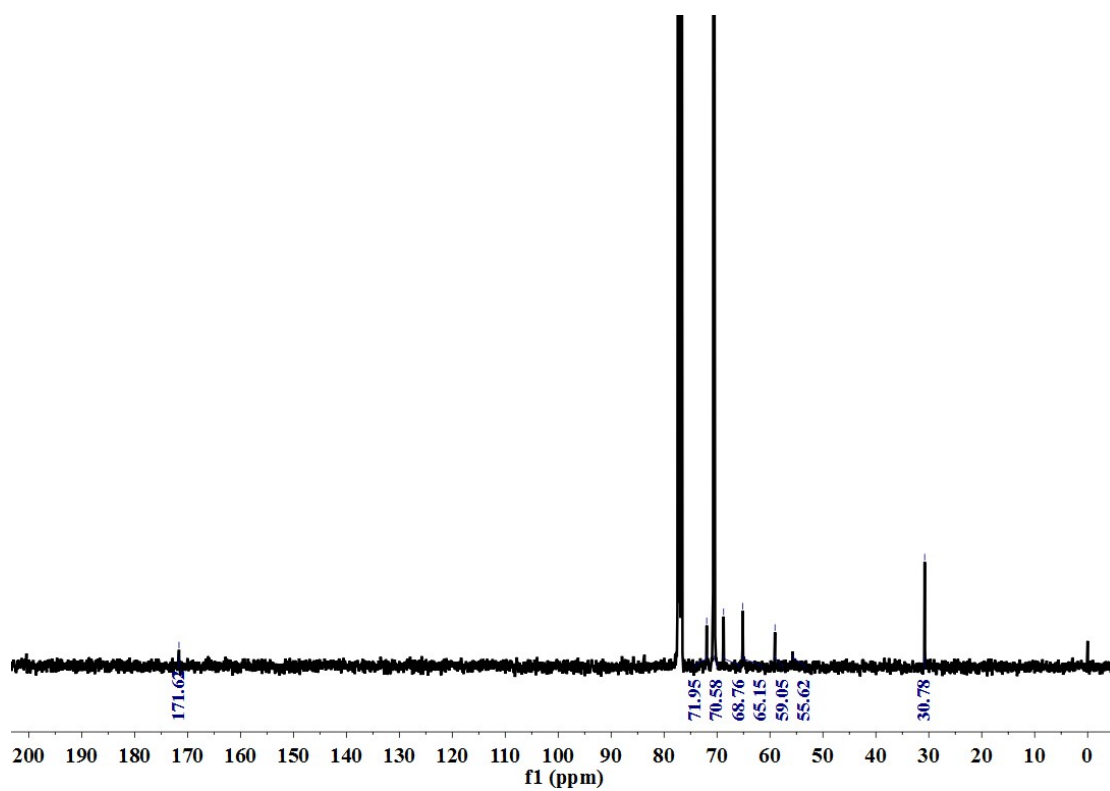


Figure S2 ¹³C NMR spectrum of PEO5000-Br

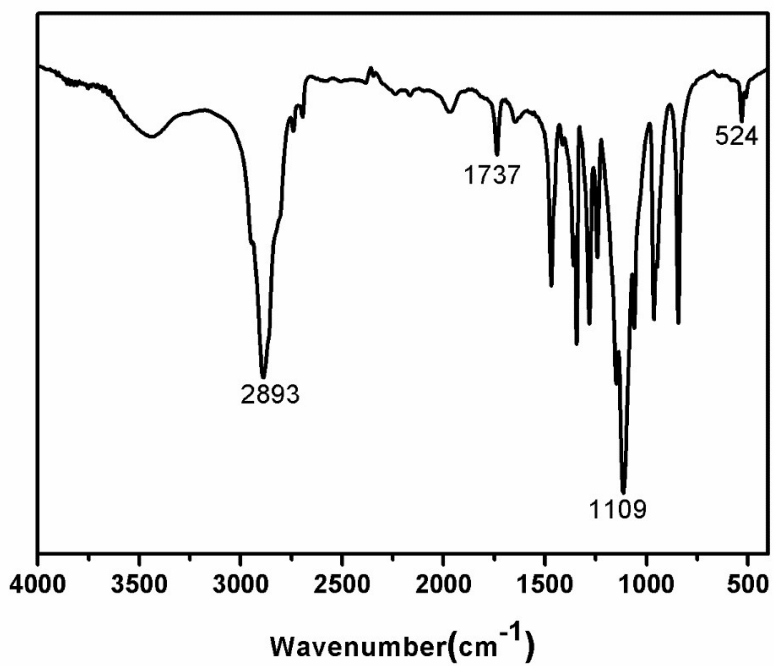


Figure S3. FTIR spectrum of PEO5000-Br

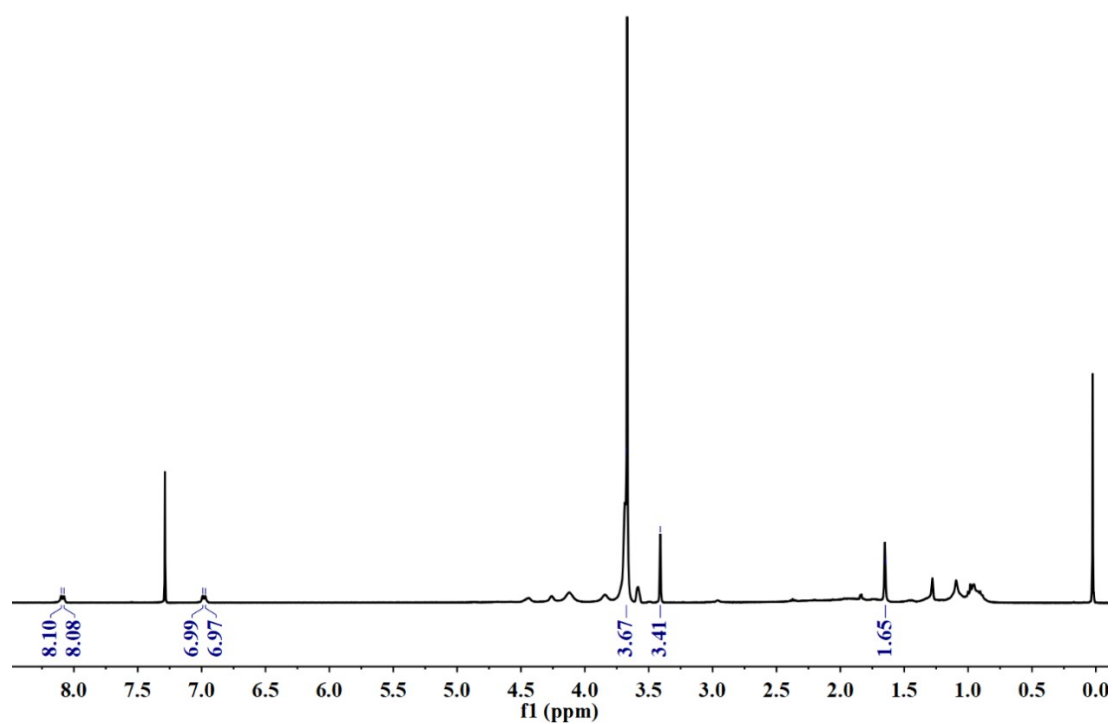


Figure S4. ¹H NMR spectrum of NG-300-2959

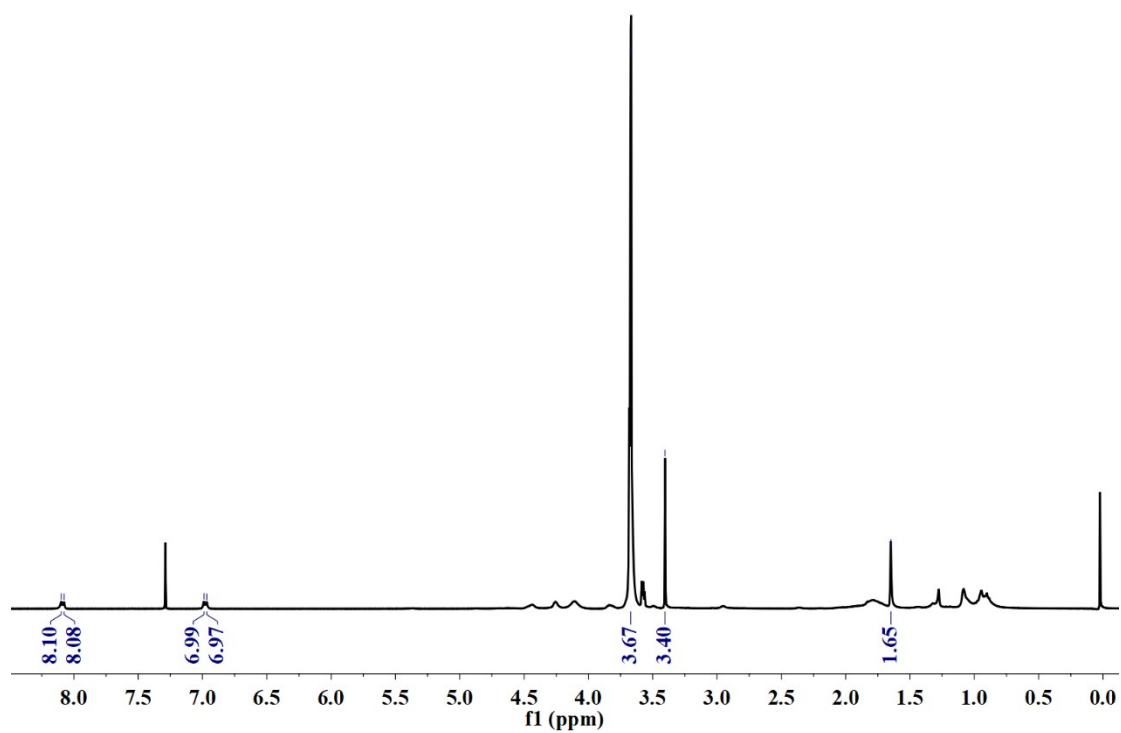


Figure S5. ¹H NMR spectrum of NG-500-2959

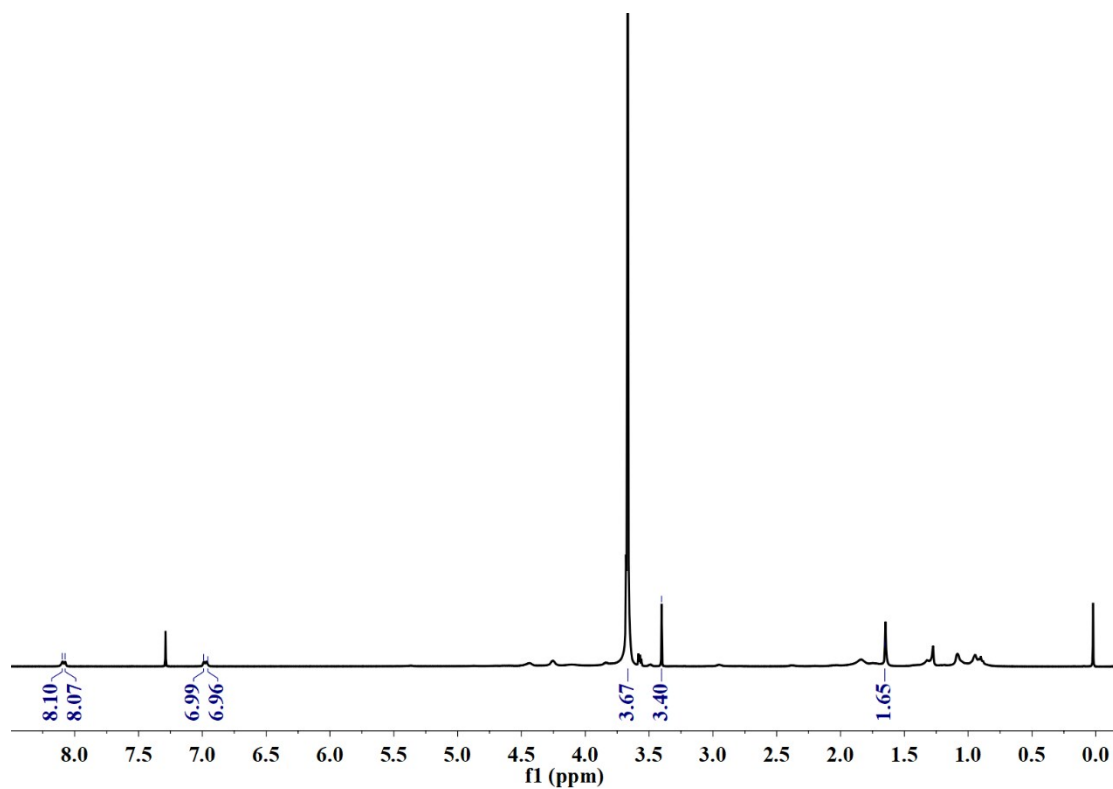


Figure S6. ¹H NMR spectrum of NG-950-2959

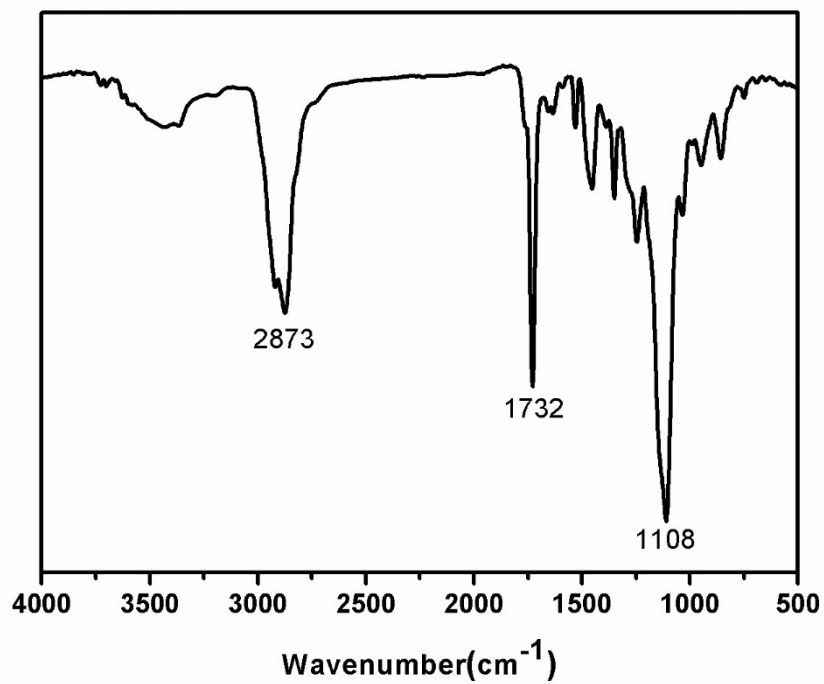


Figure S7. FTIR spectrum of NG-300-2959

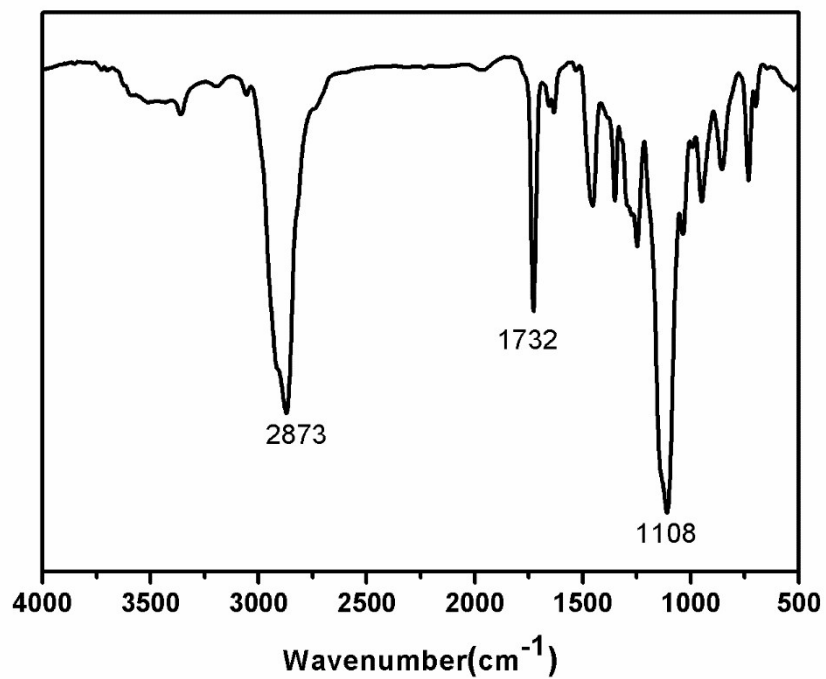


Figure S8. FTIR spectrum of NG-500-2959

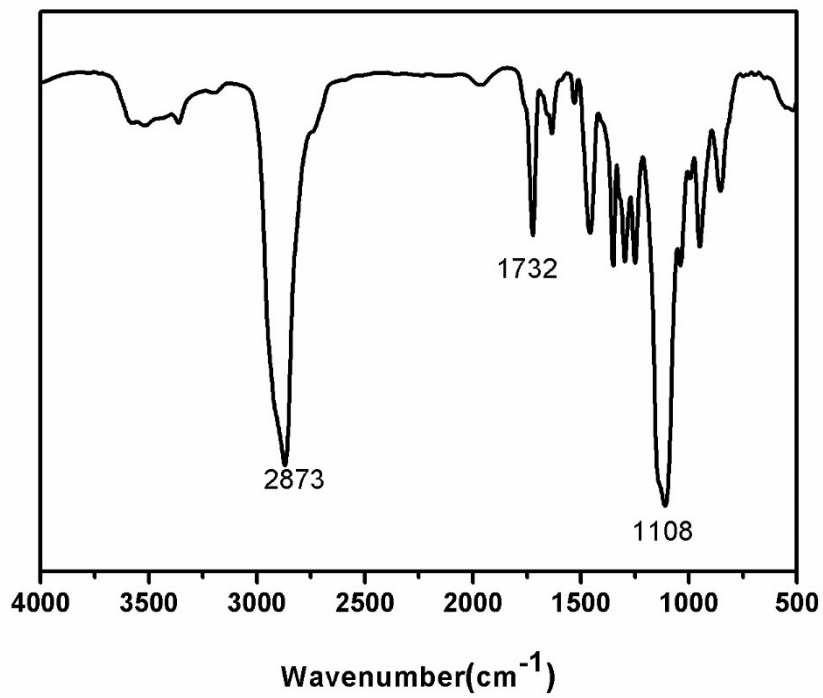


Figure S9. FTIR spectrum of NG-950-2959

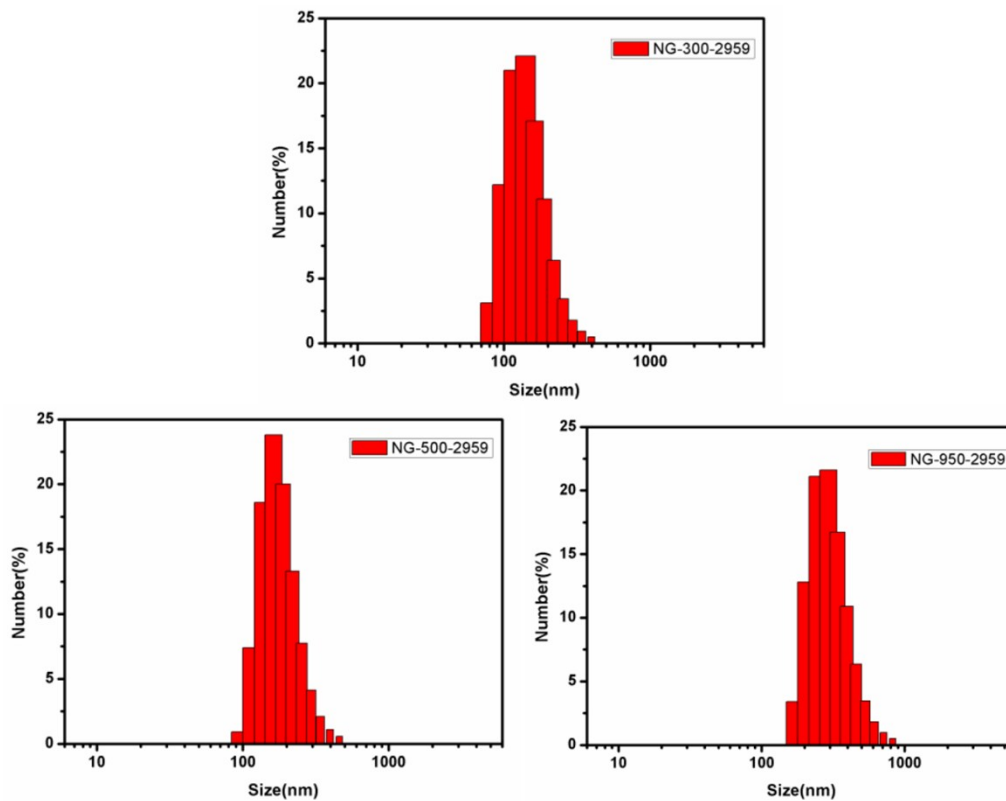


Figure S10. DLS histograms of nanogels in deionized water

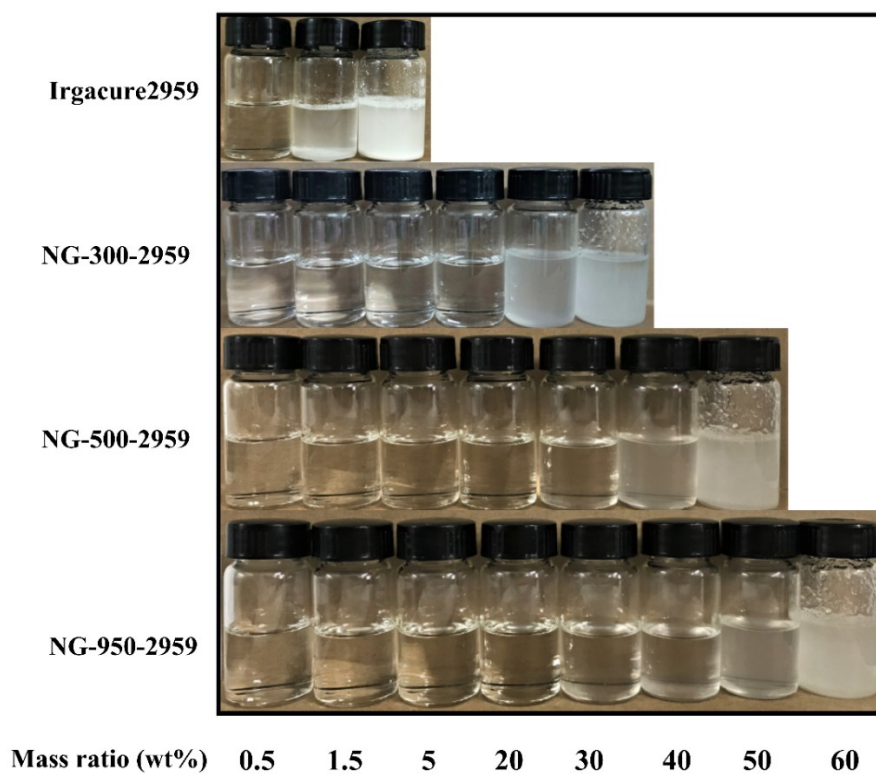


Figure S11. The images of aqueous solutions

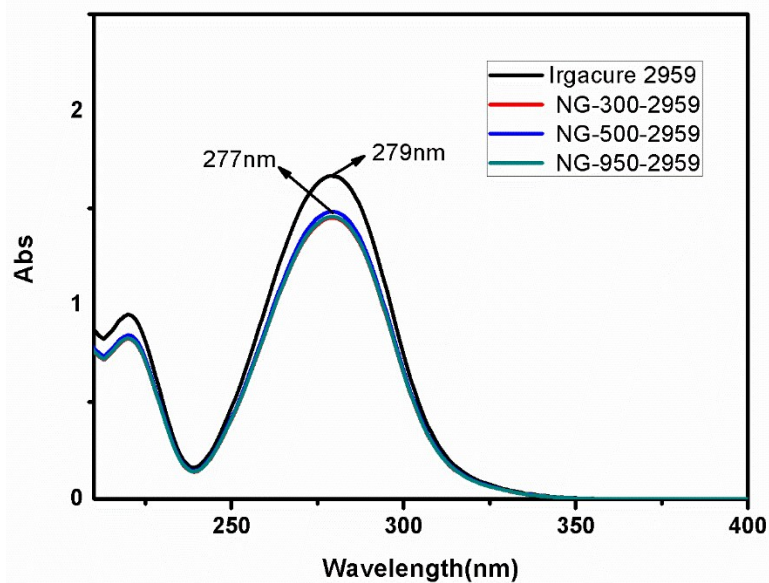


Figure S12. UV-vis absorption curves of three nanogels and Irgacure 2959 in deionized water ($C_{2959 \text{ group}} = 1 \times 10^{-4} \text{ mol L}^{-1}$)

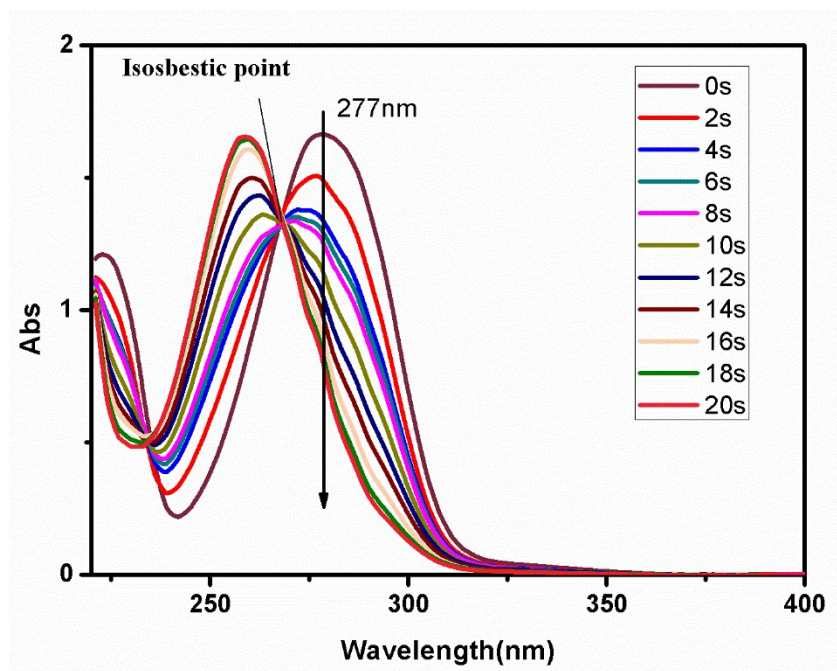


Figure S13. UV-vis degradation curves of NG-950-2959 in deionized water ($C_{2959 \text{ group}} = 1 \times 10^{-4} \text{ mol L}^{-1}$)

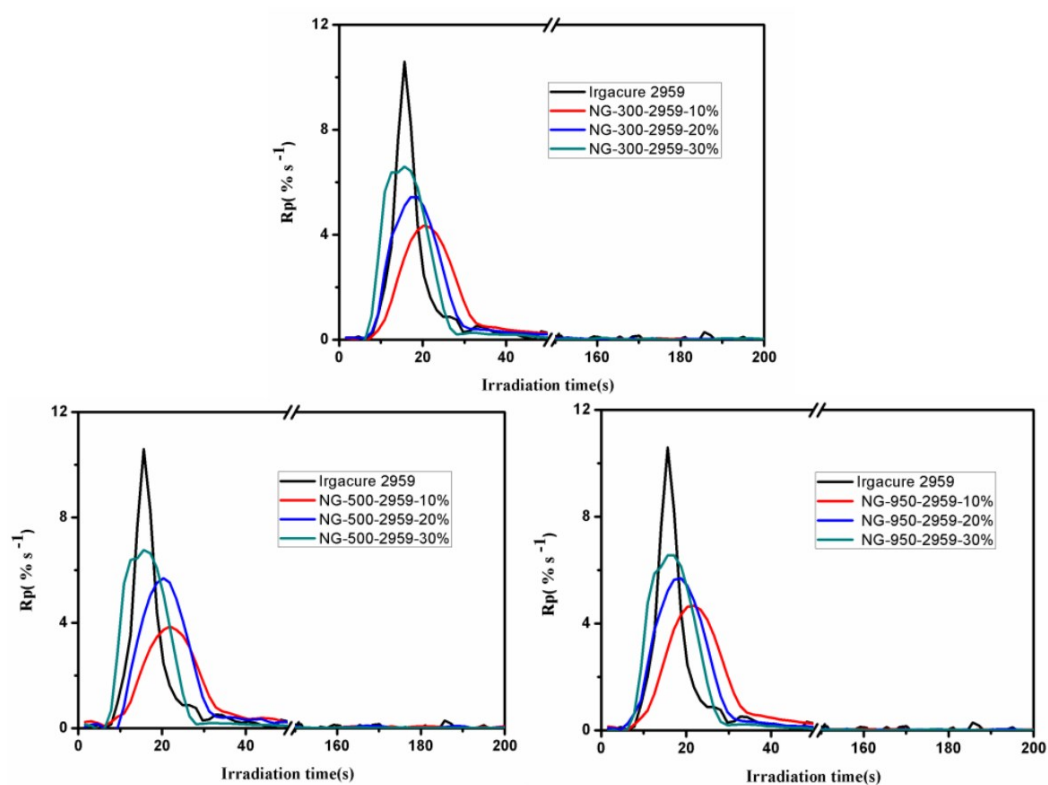
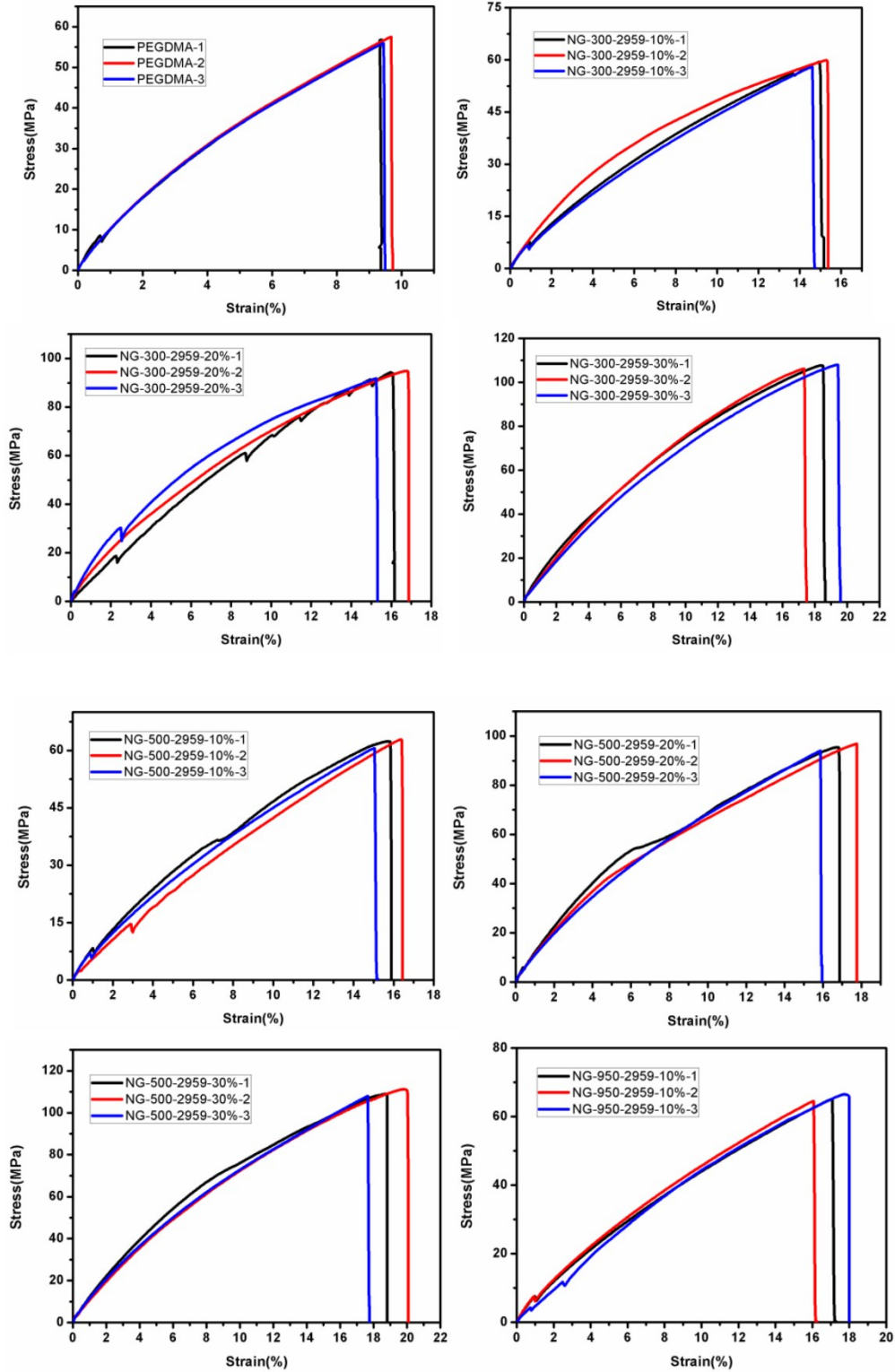


Figure S14. Polymerization rate profiles of PEGDMA initiated by the nanogels at various loading levels



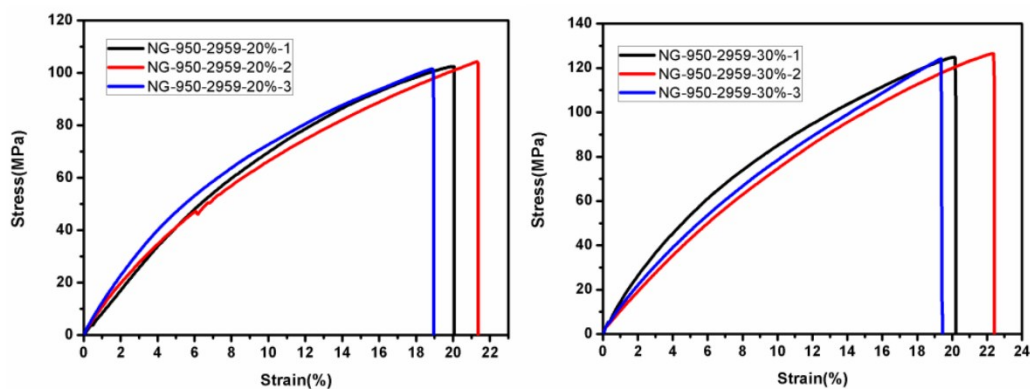


Figure S15. Stress–strain curves of cured films with different contents of nanogels

Table S1. Thermal decomposition parameters of cured films with different contents of nanogels

Photocured films	T _{5%} (°C)	T _{max1} (°C)	T _{max2} (°C)
PEGDMA	262	327	420
NG-300-2959-10%	280	345	413
NG-300-2959-20%	276	342	406
NG-300-2959-30%	262	332	403
NG-500-2959-10%	272	343	418
NG-500-2959-20%	262	345	414
NG-500-2959-30%	269	343	412
NG-950-2959-10%	276	345	417
NG-950-2959-20%	276	346	414
NG-950-2959-30%	267	334	414

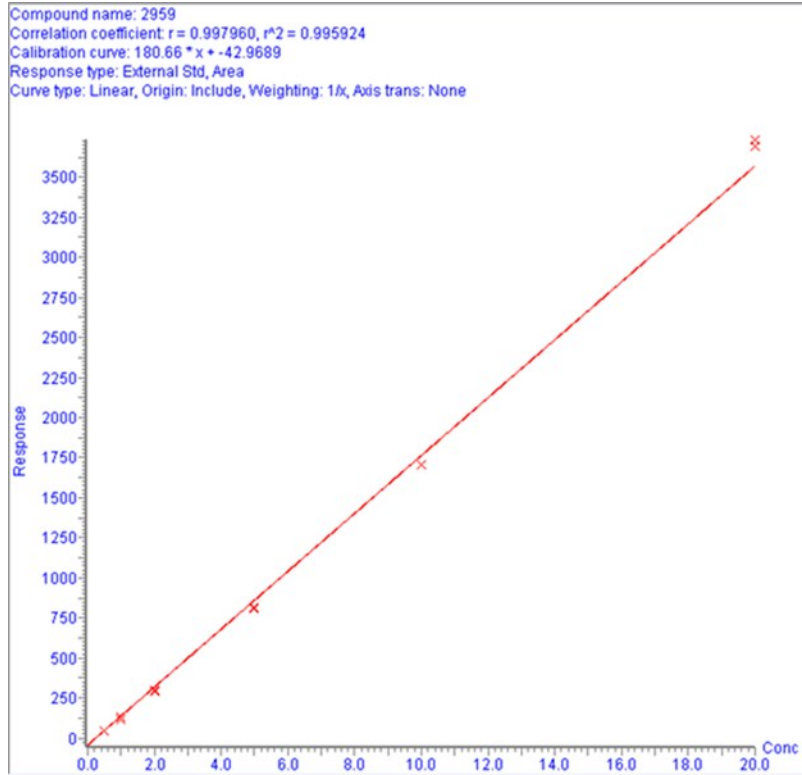


Figure S16. Standard curve of Irgacure 2959

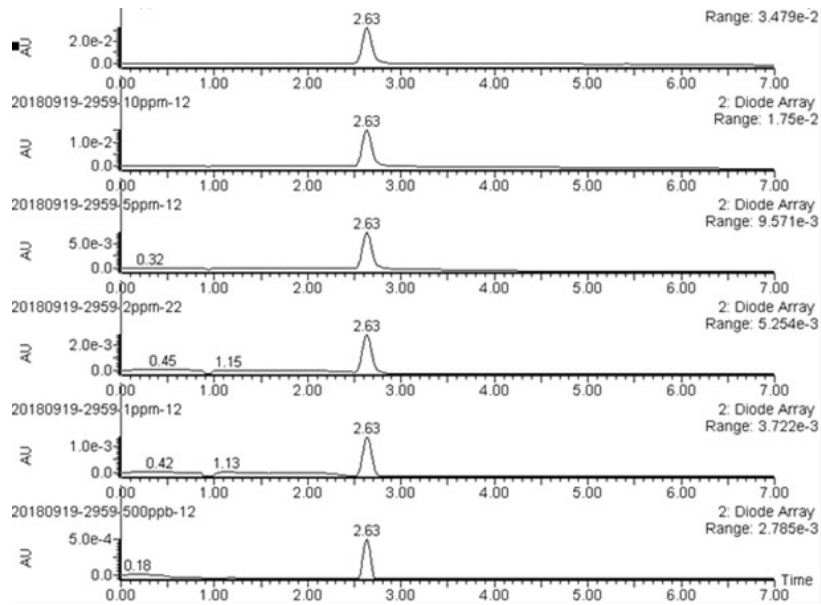


Figure S17. Chromatogram of Irgacure 2959

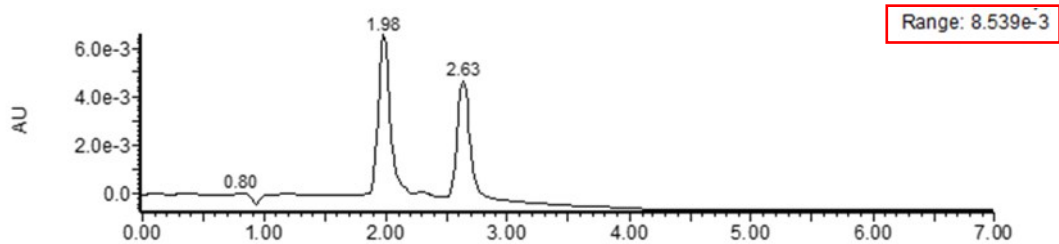


Figure S18. Chromatogram of the extraction solution of the cured film initiated by Irgacure 2959

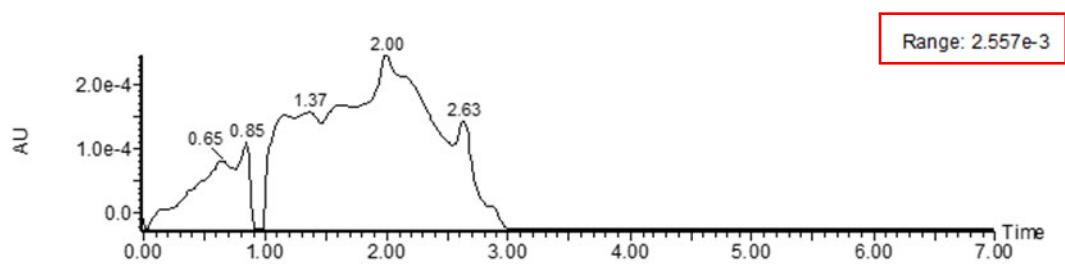


Figure S19. Chromatogram of the extraction solution of the cured film initiated by NG-950-2959

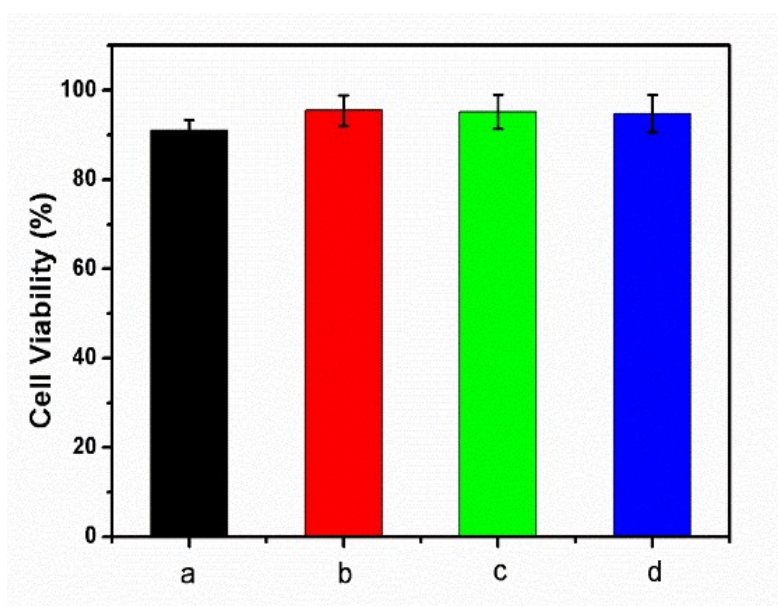


Figure S20. Viability of cured films with NG-950-2959 at different content incubated with Hela cells for 24h. a) Irgacure 2959 with the photosensitive group content equaling to that of nanogel at 10 wt% content. b) nanogel at 10 wt% content. c) nanogel at 20 wt% content. d) nanogel at 30 wt% content.